Application of nanomagnetic-hydroxyapatite in removal of Cd ions from their aqueous solutions

S. A. Abo-El-Enein, [1] H. A. El boraey, [2] R. M. El-korashy, [3]A. A. Sery [3*]

(1) Chemistry Department, Faculty of Science, Ain Shams University, Egypt

(2) Chemistry Department, Faculty of Science, Menoufia University, Egypt

(3) National Water Research Center, CLEQM, Egypt

* Corresponding author Tel.: 01110208950

E-mail address: chem_alaa.asem@yahoo.com

Abstract

Nanomagnetic-hydroxyapatite (NMHAp) has been synthesized and characterized by means of FTIR and TEM analysis. The sample was tested for the removal of Cd^{2+} ions from their aqueous solutions using batch method. The presence of magnetic particles facilitates the recovery of adsorbent after adsorption process. The specific surface area of the prepared sample is about 58 m^2/g. The uptake value obtained was 80.72 mg/g. Results showed that the Langmuir isotherm better fits sorption data than Freundlich model. Factors influencing the removal percent as pH, contact time, adsorbent dose and initial metal ion concentration have been discussed.

Keywords:

Nanohydroxyapatite-Magnetite; Langmuir isotherm; Adsorption; Water treatment.

1. Introduction

Water pollution is the contamination of water bodies (e.g. lakes, rivers, oceans ….. etc). The contamination of water by heavy metal ions arising from mining operations, textile industries, metal plating, tannery, etc., is a major environmental problem. As the large quantities of heavy metals resulted from discharge of industrial waste into the natural environment e.g. irrigation of agricultural fields by using sewage has resulted in a number of environmental problems [1] and due to their non-biodegradability and persistence, can accumulate in the environment elements such as food chain, and thus may pose a significant danger to human health [2]. There are many methods that are being used for removal of heavy metal ions include chemical precipitation, evaporation, filtration, electrolysis, reverse osmosis and Ultraviolet light [3]. Adsorption process appears to be the most effective, especially for effluents with moderate and low concentrations. It

has received more attention and increasing application due to a lot of factors: simplicity of design, high efficiency with high uptake capacity and low cost during the multi-adsorption interaction processes [4].

Application nanotechnology in the field of water purification, nanotechnology gives the possibility of an efficient removal of pollutants. Nanotechnology is the engineering of manipulating matter at the nanoscale (1-100 nm) at least one dimension [5]. At this scale, materials possess novel size-dependent properties which are different from their large counterparts due to its high specific surface area. Magnetic nanoparticles are a class of nanoparticle which can be manipulated using magnetic field gradients. Such particles commonly consist of magnetic elements such as iron, cobalt and nickel and their chemical compounds. The magnetic nanoparticles have been recently the focus of much research because they possess attractive properties which give potential use in catalysis including nanomaterial-based catalysts, biomedicine, tissue specific targeting, magnetically tunable colloidal photonic crystals, microfluids, magnetic resonance imaging, magnetic particle imaging [6], data storage [7], environmental remediation, nanofluids, optical filters and cation sensors. The physical and chemical properties of magnetic nanoparticles largely depend on the synthesis method and chemical structure [8].

Hydroxyapatite (HAp) is one of the most popular phosphates, with chemical formula $Ca_{10}(PO_4)_6(OH)_2$. The common crystal phase is hexagonal, but the monoclinic phase can be present [9]. HAp can be synthesized in the laboratory by many methods including the sol-gel process [10], hydrothermal synthesis [11], microwave synthesis [12], ultrasonic spray pyrolysis [13], wet precipitation [14], emulsion system synthesis and sonochemical synthesis [15].

The specific properties of NHAp are related to various surface characteristics, e.g., surface functional groups, acidity and basicity, surface charge, hydrophilicity and porosity. HAp has been used for the removal of many pollutants from contaminated soils and wastewater [16, 17]. Magnetic separation technique is an efficient, fast and economical method for separating magnetic materials. The main advantage of this technology is that it can dispose a mass of wastewater in a very short period of time and produce no contaminants. Nanomagnetic-hydroxyapatite (HAp/Fe_3O_4) has been prepared for the purpose of removing lead ions [18], and Zn^{2+} ions [19] from aqueous solutions.

The objective of this study is to investigate the removal efficiency of nanomagnetic-hydroxyapatite NMHAp as an alternative adsorbent material for the removal of Cd^{2+} ions from aqueous solutions.

2. Experimental

2.1. Chemicals

Calcium nitrate tetrahydrate, $Ca(NO_3)_2.4H_2O$, di-ammonium hydrogen-phosphate, $(NH_4)_2HPO_4$, ammonia solution and NH_4OH, were used for the synthesis of NHAp powder. In addition, Ferric chloride $FeCl_3$, Cupper chloride $CuCl_2$, Cetyl trimethylammonium bromide, CTAB and sodium hydroxide NaOH were used for the synthesis of cupper ferrites. cadmium sulfate octahydrate and $3CdSO_4 \cdot 8H_2O$ were used as sources of Cd^{2+}.

2.2. Synthesis of HAp nanopowder and nanomagnetic particles:

2.2.1. Synthesis of nano-hydroxyapatite powder:

Nano-HAp, $Ca_{10}(PO_4)_6(OH)_2$, was synthesized via solution-precipitation method [20]. In this method $Ca(NO_3)_2.4H_2O$ and $(NH_4)_2HPO_4$ are used as starting materials and ammonia solution for pH adjustment. The pH was kept 11 in all experiments using ammonia suspended solution. In The next step nano-HAp was precipitated and removed from the solution by centrifugation at speed of 3000 rpm then the precipitate was dried at a temperature of 100 ºC.

$$10\ Ca(NO_3)_2.4H_2O + 6\ (NH_4)_2HPO_4 + 8\ NH_4OH \longrightarrow Ca_{10}(PO_4)_6(OH)_2 + 20\ NH_4NO_3 + 20\ H_2O$$

2.2.2. Synthesis of nanomagnetic-hydroxyapatite:

Cupper ferrite is synthesized according to the sol-gel method. $CuFe_2O_4$ was prepared using $CuCl_2$ and $FeCl_3$. Then add 5 g of CTAB dissolved in 100 mL hot water. The mix was stirred for one hour. Then 1M NaOH was added drop by drop till brown solution was formed and the pH was kept at 9. This sol was stirred for about 2 hours. The next step is aging for 5-days. The mix was filtrated and washed several times with distilled water. The final precipitate was dried at 100 ºC. The dried sample was calcined at 550 ºC. A ratio of (1: 9 g) of (Cu. ferrite: NHAp) suspended in 50 mL of distilled water then stirred in ultrasonic bath for an hour then it was filtrated and dried at 100 ºC.

2.3. Characterization of NMHAp adsorbent:

The FT-IR spectra of the synthesized materials were recorded on a Pye-Unicam Sp-883 Perkins-Elmer spectrophotometer between 4000 and 400 cm^{-1} using KBr pellet technique. The nanostructure of NMHAp powder was studied using high resolution transmission electron microscopy (HRTEM) after drying at 100 ºC.

2.4. Uptake experiments:

2.4.1. Effect of initial metal ion concentration

The effect of initial metal ion concentration on the removal percent was examined at fixed adsorbent dose (0.05 g/ 50 mL) and fixed temperature (25^{o}C) shaked at ١٣٥ rpm. The residual concentration of each metal ion through Inductively Coupled Plasma (ICP), Optima 5300 DV-Perkin-Elmer. The percent heavy metal ions removal was calculated using the following equation:

$$\% \textbf{ Removal} = \frac{(C_0 - C_e)}{C_0} \times 100 \qquad (1)$$

where, C_0 is the initial concentration of metal ion (mg L^{-1});

C_e is the metal ion concentration after adsorption (mg L^{-1}).

The adsorption capacity of the adsorbent, q_e (mg metal per g dry adsorbent) can be calculated from the equation:

$$q_e = (C_0 - C_e)\frac{V}{w} \qquad (2)$$

where, V (in liter) is the solution volume and w (in gram) the amount of dry adsorbent.

2.4.2. Effect of initial pH

Adsorption of Cd^{2+} on NMHAp adsorbents under controlled pH was carried out using 0.05 g of dry adsorbent in a series of flasks each contains 50 mL of a specific metal ion solution of concentration 40 ppm. The pH was adjusted using 0.01M HCl and 0.01M NaOH.

2.4.3. Effect of contact time

The effect of contact time on the uptake of Cd^{2+} by NMHAp adsorbent was investigated using 0.05 g of dry adsorbent in a series of flasks each containing 50 mL of a specific metal ion solution and the natural pH of metal ion solutions. The contents of the flasks were shacked on a vibromatic shaker at 25±1 ºC. The samples were taken at predetermined time intervals ranging from 5 to 120 min. The residual concentration of the metal ion was determined as reported before.

2.5.4. Effect of ionic strength

Different values of Potassium chloride KCl (0.1-0.5 g/50 mL, 0.05 g adsorbent) were added to metal ions solutions with affixed concentration of each metal ion. After 60 min of continuous shaking, the solutions were centrifuged and then filtered.

2.5.5. Effect of dosage

Experiments were carried out taking different amounts of nano-adsorbent (0.025, 0.05, 0.075 and 0.1 g /50 mL) keeping the heavy metal ion parameters constant.

3. Results and discussion

3.1. Characterization of nanomagnetic-hydroxyapatite adsorbent

The FTIR spectrum of NMHAp powder was scanned in the range of 4000-400 cm^{-1}. IR spectra indicate that all spectra possess broad bands near 3500-3300 and 1629 cm^{-1} due to strongly adsorbed and/or bound water in the adsorbent materials. A strong band appears at 3437.3 cm^{-1} for NMHAp which is due to the vibrational of hydroxyl ions; the peak appeared at 1034 cm^{-1} is attributed to stretching vibrations of PO_4^{3-} while the bands located at 1384, 602 and 564 cm^{-1} are corresponding to the bending vibrations of PO_4^{3-}. The data obtained are given in **Table 1** and shown in **Fig. 1**.

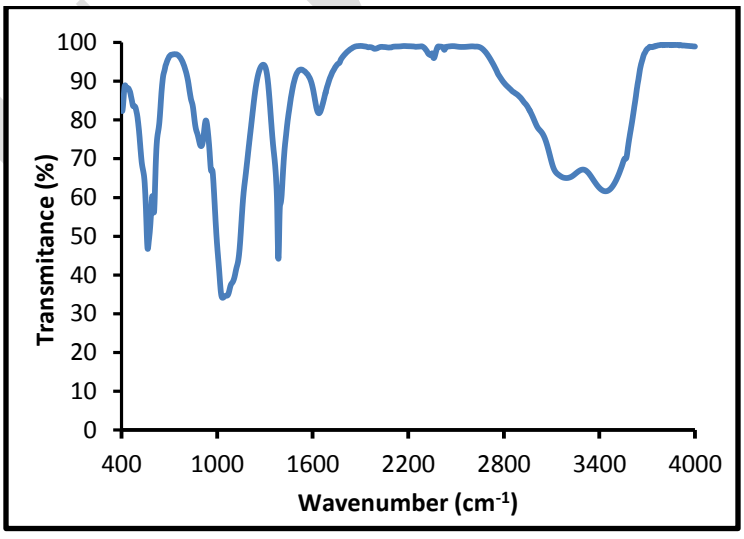

Fig. 1. FTIR spectra of nanomagnetic-hydroxyapatite

Table (1): Assignments of observed vibrational frequencies of NMHAp powder.

Assignments	NMHAp
Structural OH^-	3437.3
H_2O absorbed	1627.9
PO_4^{3-} bend ν_3	1384.2
PO_4^{3-} stretch ν_1	1034.1
PO_4^{3-} bend ν_4	602.3
PO_4^{3-} bend ν_4	564.0

The morphology and nanostructure of NMHAp adsorbents is studied using high-resolution transmission electron microscopy (HRTEM). The results of HRTEM obtained for NMHAp indicate the presence of some needle-like particles of NHAp with one main difference the agglomeration of nearly cubic particles having sizes 28-45 nm together with small particles of NHAp shielded with magnetite as shown in **Fig. 2**.

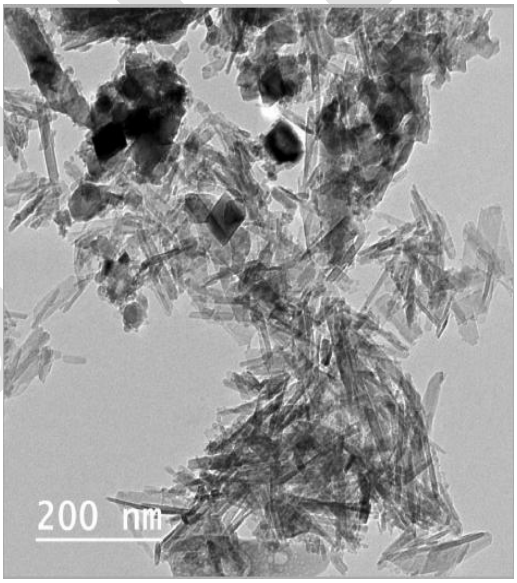

Fig. 2. HRTEM micrographs of NMHAp

3.2. Adsorption studies

Factors influencing the removal heavy metal ions removal from their aqueous solutions were investigated to properly choose the optimizing parameters of the adsorption process.

3.2.1. Effect of initial Metal ion concentration on metal Ion uptake

The metal ions uptake mechanism is particularly dependent on the initial heavy metal ions concentration; at low concentrations, metals are adsorbed by specific active sites, while with increasing metal ion concentrations the specific sites are saturated. **Fig. 3** shows the plot of experimental data points for the adsorption of Cd ions on NMHAp as a function of equilibrium concentration (C_e) at different initial metal ion concentrations. As shown, the q_e-values increase with increasing initial metal ion concentration. The maximum equilibrium q_e-values obtained for Cd (II) on nanomagnetic-hydroxyapatite are 80.7 mg/g. These results confirmed that the initial heavy metal ions concentration played an important role in the adsorption onto MHAP surface.

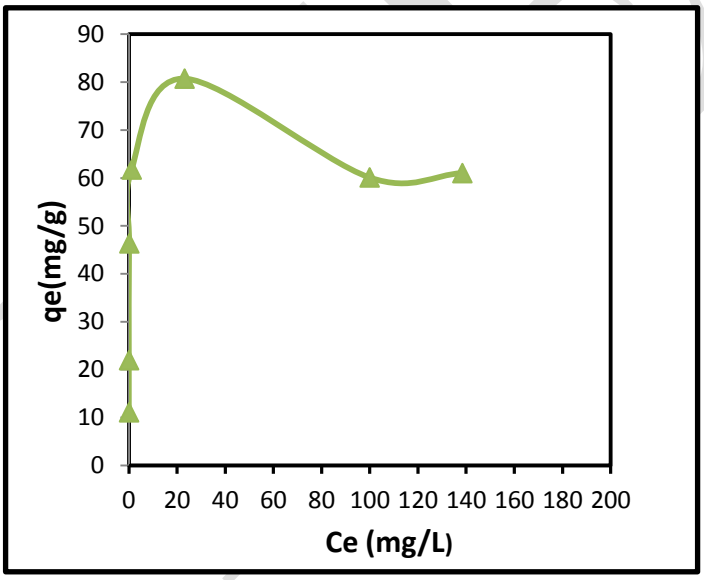

Fig. 3. Effect of initial metal ion concentration on the uptake of Cd (II) using NMHAp as adsorbent at 25ºC.

3.2.2. Effect of pH on metal ion uptake

Hydrogen ion concentration is one of the most essential parameters in the adsorption study that affect the adsorption behavior of heavy metal ions in aqueous. Adsorption of different metal ions

on the adsorbent materials under consideration was studied at varying pH values to optimize the maximum metal ion removal.

The pH dependence on metal ion uptake is due to solubility of metal ions and the ionization state of the various functional groups (carboxylate, hydroxyl, phosphate and amino groups) on the surface. NMHAp has functional groups (PO_4^{-3} and OH^-) which carry negative charges that allow the adsorbent to be potential binding sites for cations [21]. The removal of Cd (II) is about 69.2% at pH=3. The relationship between pH and metal ion removal is shown in **Fig. 4**. Since high proton concentration at lower pH, heavy metal ion uptake was decreased due to the positive charge density on metal ion binding sites. Namely hydrogen ions effectively compete with metal ions to bind the sites. The negative charge density on the cell surface increases with increasing in pH due to de-protonation of binding sites. The metal ions then become more competitive against to bind the sites which increases the metal ion uptake [22]. The removal of Cd (II) increases to about 97.1% at pH=7. Studies beyond pH=8 for cadmium ions were not attempted because precipitation of the ions as hydroxides is expected [23, 24].

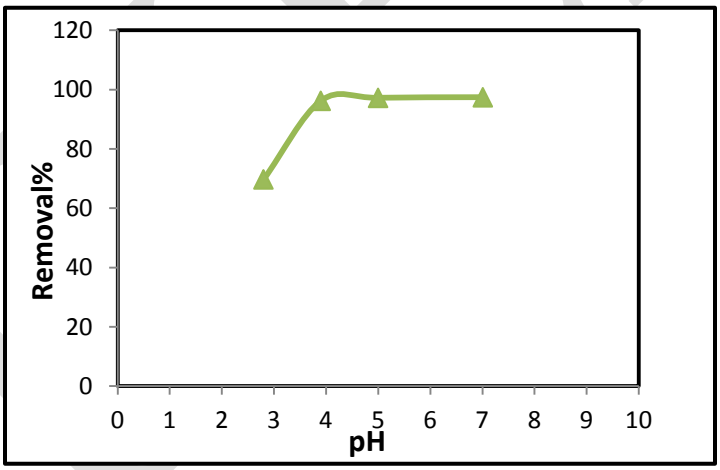

Fig. 4. Effect of pH on the removal percent of Cd (II) on NMHAp at 25ºC.

3.2.3. Effect of contact time on metal ion uptake

Equilibrium time is an important parameter for an economical wastewater treatment system. In general for a given concentration, the amount of metal ion adsorbed increases rapidly with time at the beginning, then non-linearly at a slower rate and finally attain saturation at equilibrium time, which is dependent on concentration for each adsorbent.

The results of adsorption of metal ions on NMHAp as function of time are shown in **Fig. 5**. The percent metal ion removal increased rapidly for Cd (II) in the beginning due to the presence of a

larger number of active adsorption sites on the surface of adsorbent being available for the adsorption of the metal ions. The removal percent is about 98 % after 60 min. contact time. Evidently, the equilibrium time for this metal ion is regarded to be about 60 min. for further applications.

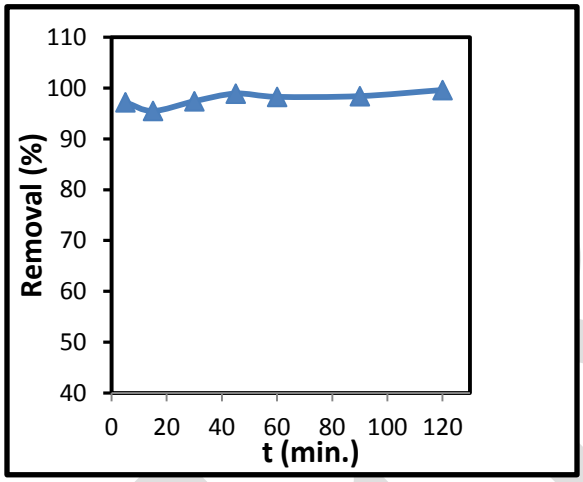

Fig. 5. Effect of contact time on the removal percent of Cd (II) on NMHAp at 25ºC.

3.2.4. Effect of adsorbent dosage on metal ion uptake

Experiments were carried out taking different amounts of nano-adsorbent keeping the heavy metal ion concentration constant in order to obtain an optimum condition as shown in **Fig. 6.** It is evident that the efficiency increases for Cd ions. The increase in the efficiency is due to an increase in the number of active sites on the surface of the different nanoparticles available for the reaction, which in turn increases the rate of adsorption [25]. The removal efficiency of cadmium ions removal increases from 90.3% to 99 % after 60 min when the adsorbent dose increases from 0.025 to 0.1 g/50 mL.

3.2.5. Effect of salinity on metal ion uptake

Generally, adsorption decreases with increasing ionic strength of the aqueous solution [26]. The electrostatic attraction at low ionic strength appears to play a negligible role in the removal of metal ions for sorbent. The results for NMHAp as adsorbent indicate that there was a slight decrease in the removal of Cd (II) ions from 95% to 83% for the interval of salinity studied. Therefore, this adsorbent can be applied for heavy metal ions removal from wastewaters containing high amount of salts. The data obtained are shown in **Fig. 7**.

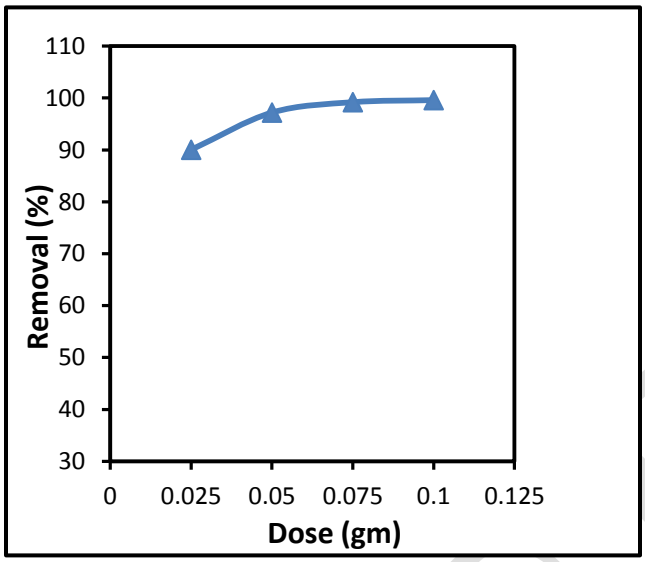

Fig. 6. Effect of adsorbent dosage on the removal percent % of Cd (II) on NMHAp at 25ºC.

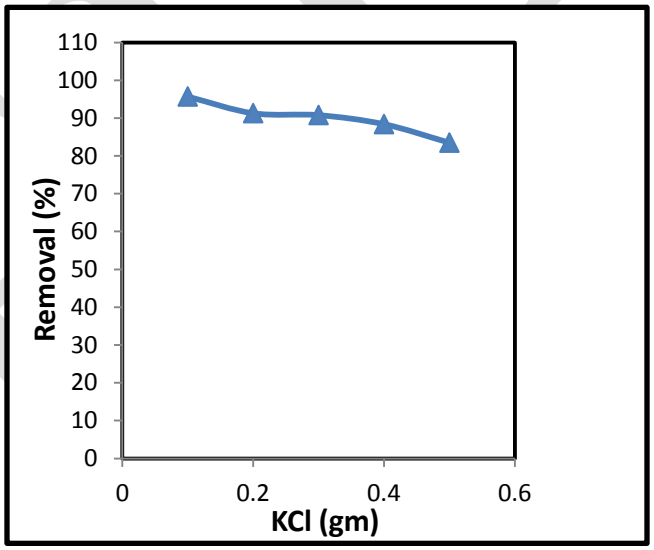

Fig. 7. Effect of salinity on the removal percent % of Cd (II) on NMHAp at 25ºC.

3.2.6. Adsorption isotherms

3.2.6.1. The Langmuir model

The Langmuir adsorption isotherm has been successfully applied to many pollutants adsorption processes and has been the most widely used sorption isotherm for the sorption of a solute from a liquid solution assuming that all adsorption sites have the same energy [27]. The isotherm can be represented as follows:

$$\mathbf{q_e} = \frac{\mathbf{Q_0 k C_e}}{\mathbf{1 + k C_e}} \quad \ldots\ldots\ldots\ldots\ldots \quad (3)$$

The above equation can be rearranged to the common linear form:

$$\frac{\mathbf{C_e}}{\mathbf{q_e}} = \frac{\mathbf{1}}{\mathbf{Q_0 k}} + \frac{\mathbf{C_e}}{\mathbf{Q_0}} \quad \ldots\ldots\ldots\ldots\ldots \quad (4)$$

Where C_e is the equilibrium concentration (mg/L); q_e is the amount of metal ion adsorbed per unit mass of adsorbent (mg/g); Q_0 is q_e for a complete monolayer (mg/g), and k is a constant related to the affinity of the binding sites (L/mg). The values of Q_0 and k for all adsorbents are determined, respectively, from slopes and intercepts of the linear plots of C_e/q_e vs. C_e. Maximum sorption capacity (Q_0) represents monolayer coverage of sorbent with sorbate.

The different adsorption parameters for the adsorption of Cd (II) on NMHAp as adsorbent are collected in **Table 2**. The plot of C_e/q_e vs. C_e, **(Fig. 8),** gives a straight line with slope and intercept of $1/Q_0$ and $1/K\ Q_0$, respectively. This indicates that the adsorption process is mainly limited to monolayer formation and proceeds according to Langmuir's isotherm. The higher the values of R^2, the more applicable the model for the metal ion examined.

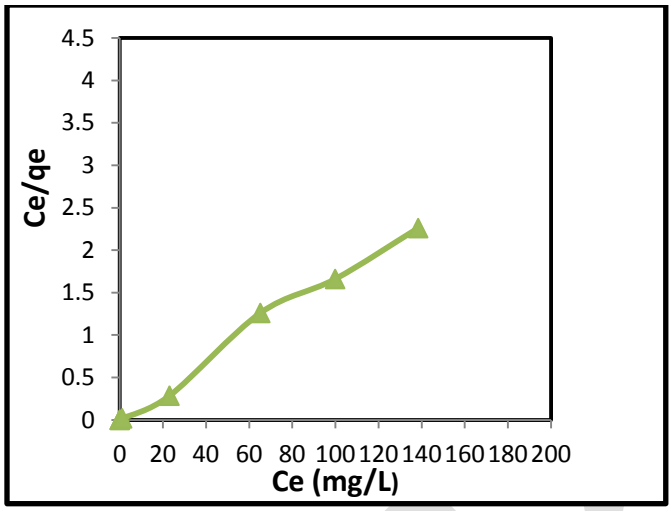

Fig. 8. Langmiur adsorption isotherms of Cd (II) on NMHAp at 25ºC.

3.2.6.2. The freundlich model

On the other hand, the Freundlich isotherm model assumes that the adsorption occurs on heterogeneous surface at sites with different energies of adsorption and with non-identical adsorption sites that are not always available [28]. Freundlich model can be represented by the linear form as follows:

$$\ln q_e = \ln K_F + \frac{1}{n} \ln C_e \quad \ldots\ldots\ldots\ldots\ldots\ldots (5)$$

where K_F is the Freundlich constant (mg/g)/ (L/mg) and n is the heterogeneity factor. The K_F value is related to the adsorption capacity; while 1/n value is related to the adsorption intensity which varies with the extent of heterogeneity of the surface of material used (adsorbent). When 1/n values are in the range $0.1 < 1/n < 1$, the adsorption process is favorable [29]**.** A plot of ln q_e versus ln C_e, gives a straight line from which the values of K_F and 1/n can be determined from the intercept and the slope, respectively. If n is below one, the adsorption is chemical process; otherwise, the adsorption is physical process [30].The value of n exceed one, suggesting the adsorption is physical process indicated from the results obtained given in **Table 2** and shown graphically in **Fig. 9**.

However, the regression coefficient of correlation R^2 values exceed 0.9 for Langmiur model while they were low for all heavy metal ions in Feundlich model indicating a deviation from linearity and suggesting that the Langmuir model is closely fitted with the experimental results obtained.

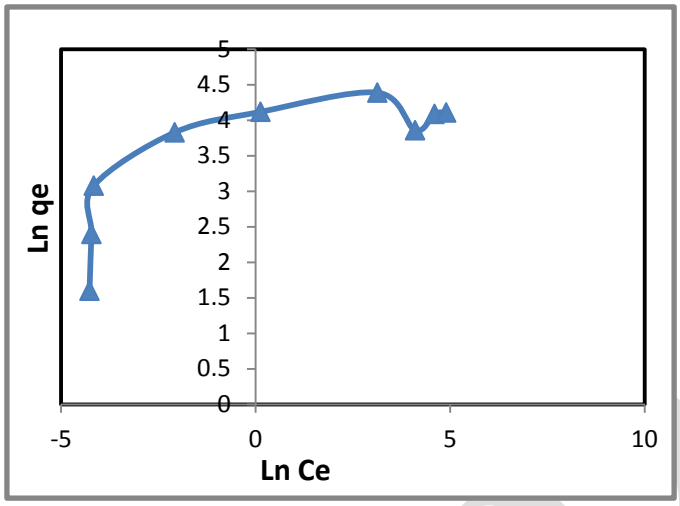

Fig. 9. Freundlish adsorption isotherms of Cd (II) on NMHAp at 25ºC.

Table (2): Adsorption isotherms parameters of Cd (II) on NMHAp.

	Langmiur isotherm			Freundlich isotherm			
Metal ion	Q_o	K	R^2	1/n	n	K_f	R^2
Cd^{2+}	59.88	0.55	0.99	0.185	5.4	31.5	0.61

3.2.7. Adsorption kinetic study

The adsorption/time data obtained were applied on two simplified kinetic models, namely like the pseudo-second-order and pseudo-first-order models as well.

3.2.7.1. Pseudo-first-order model.

The pseudo-first-order model is expressed as follows:

$$\log (q_e - q_t) = \log q_e - (\frac{k_1}{2.303})\, t \quad \text{…….. (6)}$$

where k_1 is the rate constant of pseudo-first order (min^{-1}), q_e and q_t represent the values of amount adsorbed at time (t) and at equilibrium, respectively. The kinetic parameters are

determined from the linear plots of log ($q_e - q_t$) vs. (t) as shown in **Fig. 10** and **Table 3**. The validity of the model is checked by the fitness of the straight line (R^2) as well as the consistence between experimental and calculated values of q_e. From their intercept and slope, the values K_1 and q_e are calculated.

3.2.7.2. Pseudo-second-order model

The pseudo-second-order model is expressed as follows [31]:

$$\frac{t}{q_t} = \frac{1}{k_2 q_e^2} + \frac{1}{q_e} t \quad \ldots\ldots\ldots\ldots\ldots (7)$$

where k_2 is the pseudo-second order rate constant of adsorption (g. mg^{-1}. min^{-1}), q_e and q_t (mg/g) refer to the amount of metal ions adsorbed at equilibrium and at time (t), respectively. The different kinetic parameters for the adsorption of Cd^{2+} on NMHAp surface are cited in **Table 3**. The plots of t/q_t vs. t gave straight lines for all heavy metal ions as indicated in **Fig. 11.** .

The validity of each model was checked by the fitness of the straight line (R^2). It was found that the R^2 values obtained for the pseudo-second order model are higher than those obtained for the first-order kinetic model; this indicates that the pseudo-second order model fitted with the results obtained.

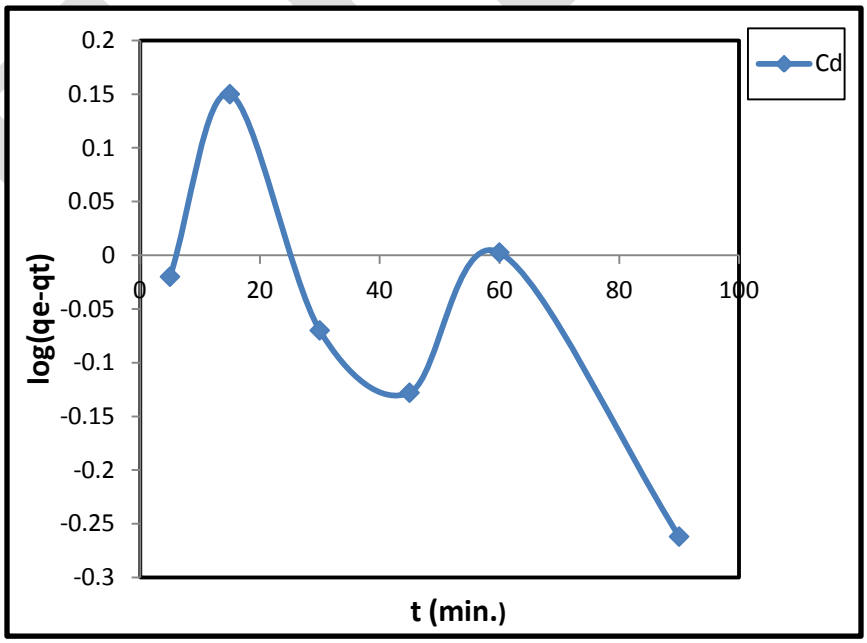

Fig. 10. Pseudo- first order kinetic model of the uptake of Cd (II) on NMHAp.

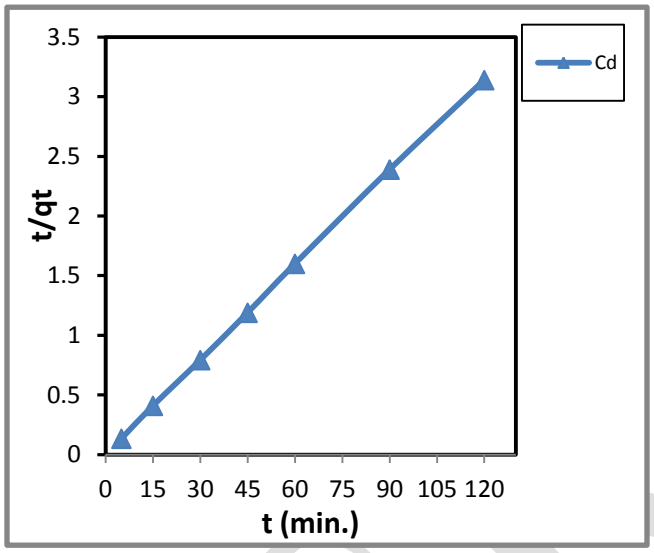

Fig. 11. Pseudo- second order kinetic model of the uptake of Cd (II) on NMHAp.

Table (3): Adsorption kinetic parameters of Cd (II) on NMHAp.

	Pseudo-second order			Pseudo-first order		
Metal ion	K_2 ($gmg^{-1}min^{-1}$)	q_e (mg/g)	R^2	K_1 $(min)^{-1}$	q_e (mg/g)	R^2
Cd^{2+}	0.0545	38.16	0.99	0.0074	1.195	0.53

4. Conclusion

In the present study, cupper ferrite has been synthesized by sol-gel method and then homogeneously mixed with nano-hydroxyapatite. The prepared composite was confirmed as an effective adsorbent for the removal of Cd (II) ions from aqueous solutions. The following results can be highlighted from the results obtained from this study:

* The specific surface area of the prepared sample is about 58 m^2/g, nanostructure of needle-like particles and with a mesoporous nature.

* The maximum equilibrium q_e-value obtained for Cd (II) on NMHAp is 80.7 mg/g.

* The pseudo-second order model is fitted with the results obtained.

* Langmiur isotherm better fits adsorption data rather than the Freundlich model.

These characteristics make NMHAp adsorbent a good candidate in the field of wastewater treatment.

References

- Kaewsarn, P. and Yu, Q. 2001. Cadmium (Ii) Removal from Aqueous Solutions by Pre-Treated Biomass of Marine Alga Padina Sp. Environmental pollution. 112, 209-213.
- Zhou, Q., et al. 2008. Biomonitoring: An Appealing Tool for Assessment of Metal Pollution in the Aquatic Ecosystem. Analytica chimica acta. 606, 135-150.
- Droste, R., Theory and Practice of Water and Wastewater Management Systems, 1997, Wiley, New York, NY.
- Zhao, X., et al. 2011. Adsorption Investigation of Ma-Dtpa Chelating Resin for Ni (Ii) and Cu (Ii) Using Experimental and Dft Methods. Journal of Molecular Structure. 986, 68-74.
- Sample, J. L. and Charles Jr, H. K. 2012. Systems Engineering at the Nanoscale. Johns Hopkins APL Technical Digest. 31, 50-57.
- Gleich, B. and Weizenecker, J. 2005. Tomographic Imaging Using the Nonlinear Response of Magnetic Particles. Nature. 435, 1214-1217.
- Hyeon, T. 2003. Chemical Synthesis of Magnetic Nanoparticles. Chemical Communications. 927-934.
- Lu, A. H., Salabas, E. e. L., and Schüth, F. 2007. Magnetic Nanoparticles: Synthesis, Protection, Functionalization, and Application. Angewandte Chemie International Edition. 46, 1222-1244.
- Marasaraju, T. and Phebe, D. 1996. Some Physicochemical Aspects of Hydroxyapatite. J. Mater. Sci. 31, 1-21.
- Andersson, J., et al. 2005. Sol–Gel Synthesis of a Multifunctional, Hierarchically Porous Silica/Apatite Composite. Biomaterials. 26, 6827-6835.
- Wang, Y., et al. 2006. Hydrothermal Synthesis of Hydroxyapatite Nanopowders Using Cationic Surfactant as a Template. Materials Letters. 60, 1484-1487.
- Liu, J., et al. 2004. Rapid Formation of Hydroxyapatite Nanostructures by Microwave Irradiation. Chemical physics letters. 396, 429-432.
- Aizawa, M., et al. 1999. Characterization of Hydroxyapatite Powders Prepared by Ultrasonic Spray-Pyrolysis Technique. Journal of materials science. 34, 2865-2873.
- Silva, C. C., et al. 2005. Hydroxyapatite Screen-Printed Thick Films: Optical and Electrical Properties. Materials Chemistry and Physics. 92, 260-268.

- Kim, W. and Saito, F. 2001. Sonochemical Synthesis of Hydroxyapatite from H 3 Po 4 Solution with Ca (Oh) 2. Ultrasonics Sonochemistry. 8, 85-88.
- Barka, N., et al. 2011. Removal of Reactive Yellow 84 from Aqueous Solutions by Adsorption onto Hydroxyapatite. Journal of Saudi Chemical Society. 15, 263-267.
- Mourabet, M., et al. 2015. Removal of Fluoride from Aqueous Solution by Adsorption on Hydroxyapatite (Hap) Using Response Surface Methodology. Journal of Saudi Chemical Society. 19, 603-615.
- Dong, L., et al. 2010. Removal of Lead from Aqueous Solution by Hydroxyapatite/Magnetite Composite Adsorbent. Chemical Engineering Journal. 165, 827-834.
- Feng, Y., et al. 2010. Adsorption of Cd (Ii) and Zn (Ii) from Aqueous Solutions Using Magnetic Hydroxyapatite Nanoparticles as Adsorbents. Chemical Engineering Journal. 162, 487-494.
- Valsami-Jones, E., et al. 1998. The Dissolution of Apatite in the Presence of Aqueous Metal Cations at Ph 2–7. Chemical Geology. 151, 215-233.
- Yin, P., et al. 1999. Biosorption Removal of Cadmium from Aqueous Solution by Using Pretreated Fungal Biomass Cultured from Starch Wastewater. Water Research. 33, 1960-1963.
- Kapoor, A., Viraraghavan, T., and Cullimore, D. R. 1999. Removal of Heavy Metals Using the Fungus Aspergillus Niger. Bioresource technology. 70, 95-104.
- Apiratikul, R., et al. 2004. Biosorption of Binary Mixtures of Heavy Metals by Green Macro Alga, Caulerpa Lentillifera. Songklanakarin J. Sci. Technol. 26, 199-207.
- Morgan, B. and Lahav, O. 2007. The Effect of Ph on the Kinetics of Spontaneous Fe (Ii) Oxidation by O 2 in Aqueous Solution–Basic Principles and a Simple Heuristic Description. Chemosphere. 68, 2080-2084.
- Gupta, V. K., et al. 2012. Photo-Catalytic Degradation of Toxic Dye Amaranth on Tio 2/Uv in Aqueous Suspensions. Materials Science and Engineering: C. 32, 12-17.
- Baker, H. M., Massadeh, A. M., and Younes, H. A. 2009. Natural Jordanian Zeolite: Removal of Heavy Metal Ions from Water Samples Using Column and Batch Methods. Environmental monitoring and assessment. 157, 319-330.
- Langmuir, I. 1916. The Constitution and Fundamental Properties of Solids and Liquids. Part I. Solids. Journal of the American Chemical Society. 38, 2221-2295.
- Walker, G. and Weatherley, L. 2001. Adsorption of Dyes from Aqueous Solution—the Effect of Adsorbent Pore Size Distribution and Dye Aggregation. Chemical Engineering Journal. 83, 201-206.
- Vázquez, I., et al. 2007. Removal of Residual Phenols from Coke Wastewater by Adsorption. Journal of Hazardous Materials. 147, 395-400.

- Jiang, J.-Q., Cooper, C., and Ouki, S. 2002. Comparison of Modified Montmorillonite Adsorbents: Part I: Preparation, Characterization and Phenol Adsorption. Chemosphere. 47, 711-716.
- Guibal, E., Milot, C., and Tobin, J. M. 1998. Metal-Anion Sorption by Chitosan Beads: Equilibrium and Kinetic Studies. Industrial & Engineering Chemistry Research. 37, 1454-1463.